Crystal Poisson's Ratios of Polyethylene and Poly(vinylalcohol) Estimated by X-ray Diffraction Using the Ultradrawn Films

Chunye Xu and Masaru Matsuo*

Department of Textile and Apparel Science, Faculty of Human Life and Environment, Nara Women's University, Nara 630 Japan

Received February 11, 1998

ABSTRACT: The elastic compliances of polyethylene (PE) and poly(vinylalcohol) (PVA) crystals were measured by X-ray diffraction using the films prepared by gelation/crystallization from dilute solutions. The measurements were carried out at 20 °C for the PE and PVA films with elongation ratios of 60 and 11, respectively. For the PE films, the measurable compliances, S_{13}^c and S_{23}^c, were (−0.013 to −0.017) × 10^{-2} GPa^{-1} and (−0.040 to 0.043) × 10^{-2} GPa^{-1}, respectively, while for the PVA films, they were −0.012 × 10^{-2} and (−0.037 to −0.038) × 10^{-2} GPa^{-1}, respectively. From the above values, the corresponding Poisson's ratios, ν_{13}^c and ν_{23}^c, of PE crystals were estimated to be 0.029−0.038 and 0.090−0.096, respectively, while ν_{13}^c and ν_{23}^c, for PVA crystals are 0.026 and 0.081−0.083, respectively. A question can be arisen as to whether the crystal elastic compliance and Poisson's ratio as measured by X-ray diffraction are equal to the corresponding intrinsic values. To check this, a mathematical representation based on a linear elastic theory was proposed by which one may investigate the dependence of the crystal Poisson's ratios on molecular orientation and crystallinity. The mathematical description indicated that the crystal Poisson's ratio as estimated by X-ray diffraction are essentially different from the intrinsic crystal Poisson's ratios. Even so, the numerical calculations indicated that the values as measured by X-ray diffraction are equal to the intrinsic values, if the morphology of test specimens can be represented as a parallel model for composite of the crystal and amorphous phases, approximately.

I. Introduction

Polymer molecules are intrinsically anisotropic in physical properties (e.g., mechanical and optical). This intrinsic anisotropy causes the bulk properties of polymer aggregates to be anisotropic when the polymer molecules are oriented. For the mechanical anisotropy of the structural unit, crystal stiffnesses or crystal compliances have been estimated for inorganic and organic materials and metals by ultrasonic and Brillouin light scattering techniques. For example, the elastic properties of thin films and multilayers can be directly determined by Brillouin light scattering, since the wavelength of the acoustic phonon is comparable to the total thickness of the film. Unfortunately, these techniques cannot be applied to polymer materials which cannot form large single crystal mats. Namely, these methods are meaningless to crystalline polymer containing crystal, amorphous, and grain boundary regions. Accordingly, for polymeric systems, the crystal compliance (crystal lattice modulus) along the chain axis has been investigated by wide angle X-ray diffraction (WAXD) as an alternative way to access the elastic properties of crystallites within the specimen due to its sensitivity to the strain and stress dependence. This information have played an important role to estimate crystal lattice modulus along the chain direction corresponding to the ultimate value of Young's modulus in bulk specimens.[1−4] The crystal lattice modulus along the chain direction has been measured mainly for polyethylene by X-ray diffraction, Raman spectroscopy,[5] and inelastic neutron scattering.[6] The Raman and neutron values are slightly higher than that obtained by X-ray diffraction. This difference may be due to only the essential problem of determining in the crystal lattice modulus by Raman spectroscopy and inelastic neutron scattering. Namely, in addition to the difficulty in estimating crystal lamellar length by small angle X-ray scattering, both methods contain an unfavorable assumption concerning the frequency of absorption bands in a polymeric system. X-ray diffraction has advantage of determining crystal lattice modulus directly, if the stress homogeneous hypothesis is valid. That is, the inner stress along the chain axis in a specimen must be everywhere the same as the external stress applied along the stretching direction. The stress homogeneous hypothesis could be valid for polyethylene (PE) dry gel films with draw ratios $\lambda > 50$,[3] polypropylene (PP) dry gel films with $\lambda > 30$,[7] and poly(vinylalcohol) dry gel films with $\lambda > 10$.[8] Namely, the experimental values were almost independent of the draw ratio and were 213−229 GPa for PE,[3] 40−43 GPa for PP,[7] and 200−220 GPa for PVA.[8] In spite of a number of reports for crystal lattice modulus (the crystal elastic compliance along the chain axis),[1−8] few papers for estimating the crystal Poisson's ratios by X-ray diffraction have been reported for normally-drawn polyethylene by Miyasaka et al.,[9] poly(*p*-phenylene terephthalamide) by Nakamae et al.[10] and polydiacetylene single crystal by Tashiro et al.[11] Such few publications are due to the difficulty in measuring very small compressible (negative) crystal strain perpendicular to the direction of the external applied stress. This paper deals with the measurements of crystal elastic compliances S_{13}^c and S_{23}^c as well as Poisson's ratios ν_{13}^c and ν_{23}^c of polymer crystals using ultra-drawn PE and high-drawn PVA films to ensure the homogeneous stress hypothesis. Furthermore, a mathematical description based on a linear elastic theory is proposed by which one may investigate the dependence of the crystal Poisson's ratios as measured by X-ray diffraction on molecular orientation and crystallinity.[16,17] In this

* To whom all correspondence should be addressed.

10.1021/ma980214p CCC: $18.00
Published on Web 04/03/1999

paper, the crystal chain directions of PE and PVA are chosen as the *c* and *b* axis, respectively, to pay our respects with regards to the original paper.[1,2] Incidentally, we must introduce the original works regarding Poisson's ratios by Wool et al. which were estimated by Raman spectroscopy using stressed PE.[14,15] They determined them on the basis of the magnitude and stress-induced changes in the valence coordinate which were obtained from the conformational-energy-minimized coordinates of the PE chain section at 0 and 1.67 GPa. According to their paper,[15] Poisson's ratio, defined as the negative of the lateral contraction strain divided by the longitudinal strain, is approximately 0.16 in the direction normal to the plane of the all-trans plane of the backbone of the single PE chain, while the Poisson's ratio for contraction in the zigzag plane is 0.11. Apart from their estimation, the present paper deals with the Poisson's ratios directly from the external applied stress-crystal strain relationship without assuming any potential function.

II. Experimental Section

Sample Preparation and Characterization. Polyethylene. The sample was linear PE (Hercules 1900/90189) with an average viscosity molecular weight of 6×10^6. Gel films were prepared by crystallization from decalin solutions, the concentration being 0.45 g/100 mL, according to the method of Smith and Lemstra.[16,17] They were dried under ambient conditions. The dry gel films were cut into strips, which were elongated at 135 °C. From WAXD patterns, uniplanar orientational degree of the (200) plane parallel to the film surface became more pronounced as draw ratio (λ) increased. This tendency became considerable for the films with $\lambda > 70$. To ensure sufficient levels of diffraction intensity for accurate measurements of the lattice strain of the (200) plane, it was necessary to ensure random orientation of the (200) plane about the initial draw axis. For this purpose, the draw ratio was fixed to be 60. Even so, X-ray patterns (end view) implied that some of the drawn films took a uniplanar orientation of the (200) plane. Therefore, drawn films with circular diffraction rings were adopted as test specimens in this experiment.

The density of the films was measured by a pycnometer with chlorobenzene−toluene as a medium, and the crystallinity was determined to be about 94% using 1.000 and 0.852 g/cm^3 as densities of the crystal and amorphous phases, respectively.[23]

The second and forth order orientation factors of the *c* axis was measured from the orientation distribution function of the (002) plane for all test specimens.[3] The second-order orientation factor of amorphous chain segments was estimated by subtracting the crystalline contribution from the total birefringence.[18] The fourth-order factor of the amorphous chain segments was calculated by using an inversely superposed Gaussian type function with the parameter which gives the best value of the second order factor.[8] Detailed methods were described elsewhere.[4,19]

Poly(viny alcohol). PVA powder was used; the sample had polymerization of 17 900 and a 98% hydrolysis. PVA gels were prepared by crystallization from semidilute solutions in the dimethyl sulfoxide (Me_2SO) and water (H_2O) mixtures, the concentration being 1 g/100 mL. The Me_2SO/H_2O composition was set to be 70/30 to ensure the high drawability of PVA films based on a report by Cha et al.[20] Solutions were prepared by heating the well-blended polymer/solvent mixture at 105 °C for 40 min. The homogenized solution was poured into an aluminum tray kept at temperature >l00 °C, and then the tray was placed in a cold bath set at temperatures <−100 °C, thus generating a gel. The gels kept at temperature <−100 °C for 5 h were immersed in a water bath at 20 °C for a week to remove Me_2SO.[21,22] The gels were dried by evaporating water under ambient conditions. WAXD patterns of the dry gel films with film thickness <300 μm suggested a uniplanar orientation of the (101) plane parallel to the film surface, probably leading to planer tension during gelation and drying processes. For specimens with thicknesses >700 μm, the pattern (end view) exhibited circular diffraction rings, indicating random orientation of crystallites. The dry gel film with random crystal orientation was cut into strips of length 35 mm and width 20 mm. The strip was clamped in a manual stretching device in such a way that the length to be drawn would be 10 mm. The specimen was placed under nitrogen at 160 °C and elongated manually up to seven times. Immediately, after stretching, the stretcher with the sample was quenched to room temperature. Further elongation was done at 180 °C up to 11 times, since a temperature suitable to realize the facile drawability shifted to higher values as λ increased. Uniplanar orientation of the (101) plane appeared again by the elongation of undrawn films with random orientation of crystallites but this degree was negligible small. The density of the films was measured by a pycnometer with *p*-xylene and carbon tetrachloride as the medium. The crystallinity was 52−58%, which was calculated by assuming the densities of crystalline and amorphous phases to be 1.345 and 1.268 g/cm^3, respectively.

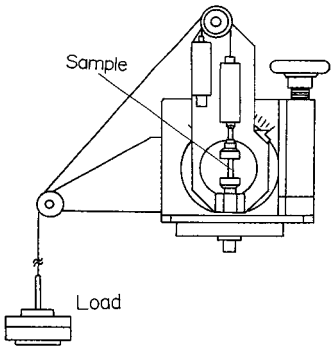

Figure 1. Apparatus to measure the Poisson ratios.

By using the method similar to PE, the second- and fourth-order orientation factors of the *b* axis (crystal chain axis) of PVA were estimated from the orientation distribution function of the (020) plane and the second- and fourth-order factors of the amorphous chain segments were obtained by the method similar to PE.

Experimental Procedure. Crystal lattice strain was observed by a 12-kW rotating anode X-ray generator (Rigaku RDA-rA operated at 200 mA and 40 kV) and monochromatized using a curved graphite monochromator. The incident beam through the monochromator was collimated by a divergent slit with $^1/_6$°. The diffraction beam was passed through a receiving slit of 0.15 mm width and scatter-slit with $^1/_6$° before reaching the counter. The diffraction intensity peaks from the crystal planes were measured at 0.02° intervals over a time period of 200 s in the desired range of $2\theta_B$ (twice the Bragg angle). The curve for calculating the center of gravity was obtained as a function of the twice the Bragg angle in the range of about ±0.2° from a peak. For example, the intensity curve for the (200) plane of PE with a peak at 24.055° under no stress was obtained as a function of twice the Bragg angles from 23.76 to 24.4°. Through trial and error, this method was confirmed to be the best one to detect the very small peak shift by external applied stress. Even so, the diffractdin intensity plots against twice the Bragg angle were scattered around a peak top for most of the test specimens, and such data must be eliminated because of the difficulty in obtaining a smooth curve. By using the plots assuring a smooth curve, the deviation of the center of gravity of intensity curve with a peak was calculated by curve fitting. Here we must emphasize that the results estimated by the shift of peak position by the curve fitting were almost equal to those by the shift of the center of the gravity. Incidentally, the value of PE crystal lattice modulus along the chain axis estimated from the deviation of the center of gravity of the intensity curve was already confirmed to be equal to that estimated from the deviation of a peak top.[3]

The drawn specimen was mounted vertically as shown in Figure 1 to measure compressible (negative) strains of the crystal planes whose reciprocal lattice vectors are perpendicu-

Table 1. Characteristics of the PE and PVA Films[a]

specimen	crystallinity (%)	F_{200}^{cry}	F_{400}^{cry}	F_{200}^{am}	F_{400}^{am}
PE	93−95	0.921−0.932	0.850−0.862	0.843−0.869	0.570−0.576
PVA	52−58	0.918−0.930	0.849−0.861	0.841−0.866	0.568−0.574

[a] F_{200}^{cry}, the second-order orientation factor of the *c* axis of PE and the *b* axis of PVA; F_{400}^{cry}, the fourth-order orientation factor of the *c* axis of PE and the *b* axis of PVA; F_{200}^{am}, the second-order orientation factor of the amorphous chain segments of PE and PVA; F_{400}^{am}, the fourth-order orientation factor of the amorphous chain segments of PE and PVA.

lar to the crystal chain axis. The friction between a steel wire and a ring was confirmed to be negligible small. Incidentally, the specimen elongation was also found to be negligible small during the measurements of the crystal strain.

For the present system, the mechanical properties of a polymeric crystal unit can be described by Hook's law relating strain ϵ to the external stress σ applied to the stretching direction of a test specimen.

$$\epsilon_{11}^c = S_{13}^c\sigma$$
$$\epsilon_{22}^c = S_{23}^c\sigma \qquad (1)$$
$$\epsilon_{33}^c = S_{33}^c\sigma$$

where S_{13}^c, S_{23}^c, and S_{33}^c are the crystal elastic compliances as measured by X-ray diffraction. Thus, the crystal Poisson's ratios, ν_{13}^c and ν_{23}^c, may be given by

$$\nu_{13}^c = -\frac{S_{13}^c}{S_{33}^c}$$
$$\nu_{23}^c = -\frac{S_{23}^c}{S_{33}^c} \qquad (2)$$

In this paper, the subscripts 3, 2, and 1 for a PE crystal unit cell are chosen in the direction of the *c*, *b*, and *a* axes, respectively. *For a PVA crystal unit cell, the subscripts 3 and 2 are chosen along the b axis (crystal chain axis) and the [002] direction, respectively. The subscript 1 is chosen along the [200] direction instead of the a-axis by considering that the angle β (=91.7°) within the crystal unit is close to 90°.*

III. Results and Discussion

Table 1 summarizes the crystallinity and the second and fourth order orientation factors of the crystal chain axis and amorphous chain segments within the PE films with $\lambda = 60$ and the PVA films with $\lambda = 11$. In spite of the large difference of draw ratio between the PE and the PVA films, the orientation factors of the crystal and amorphous chain segments of the PE films are almost equal to those of the PVA films. Incidentally, the orientation distribution function to determine the orientation factor was measured using a point-focus optical system, which has elsewhere been described.[3]

Figures 2 and 3 show compressible (negative) crystal strains measured for the [200] and [020] directions of a PE crystal unit, respectively, against the external applied stress. To check the reproducibility, measurements of S_{13}^c and S_{23}^c were carried out for 30 test specimens. The results are only the examples of three specimens showing a good straight line, because of the difficulty in obtaining a smooth curve of diffraction intensity curve against twice the Bragg angle as described in Experimental Section. Among the 30 test specimens, 10 specimens provided the smooth curve and assured a straight line of compressible (negative) crystal strain against the external applied stress. The measurements were much more difficult than that of S_{33}^c, since

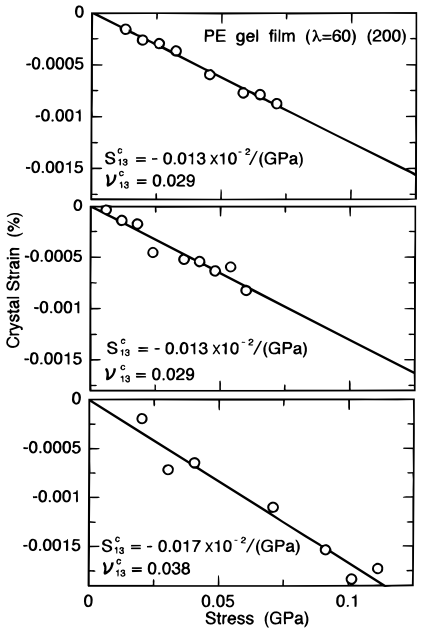

Figure 2. Crystal strain−stress relationship in the [200] direction for the PE films, when the external stress is applied to the stretching direction.

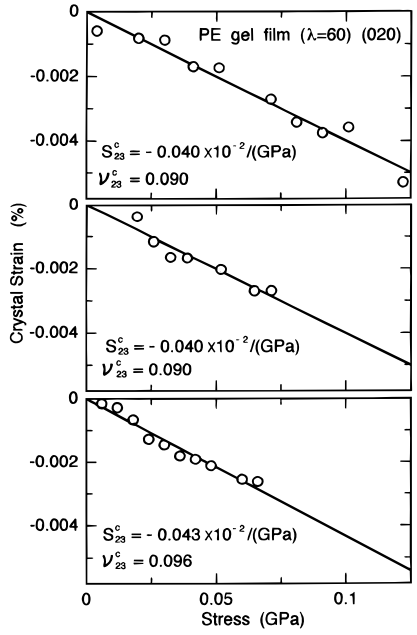

Figure 3. Crystal strain−stress relationship in the [020] direction for the PE films, when the external stress is applied to the stretching direction.

the peak shift by the compressible (negative) crystal strain is much smaller than that by the elongational (positive) crystal strain. Furthermore, we must emphasize that the external applied stress on measuring S_{13}^c and S_{23}^c was obliged to be much smaller than that on measuring S_{33}^c . This is due to the fact that the

Table 2: Reproducibility of S_{13}^c and S_{23}^c Obtained for the 10 UHMWPE Test Specimens

S_{13}^c	$\times 10^{-2}$ GPa^{-1}	−0.012	−0.013	−0.014	−0.017
	frequency	1	4	2	3
S_{23}^c	$\times 10^{-2}$ GPa^{-1}	−0.037	−0.040	−0.041	−0.043
	frequency	1	5	1	3

increase in the compressible crystal strain becomes less pronounced drastically as the applied stress increases beyond 0.12 GPa, indicating out of the framework of Hook's law. Namely, the linear relationship between the crystal strain and the applied stress could not be maintained. This implies that large applied stress is meaningless and relative small stress must be applied to test specimens on measuring S_{13}^c and S_{23}^c. Accordingly, such severe conditions as described in Experimental Section (Experimental Procedure) must be adopted. Incidentally, Table 2 showed the reproducibility of the obtained values of S_{13}^c and S_{23}^c for the 10 specimens assuring a smooth curve of the diffraction intensity against twice the Bragg angle as well as a straight line of compressible (negative) crystal strain against the external applied stress.

On the basis of the plots showing a linear relationship in the given stress range, the straight line was determined by the method of least squares. The elastic compliances S_{13}^c and S_{23}^c determined from the slope were (−0.013 to −0.017) $\times 10^{-2}$ and (−0.040 to −0.043) $\times 10^{-2}$ GPa^{-1}, respectively, in which the former and latter possibilities predicted from Table 2 are 90%. This indicates very high accuracy. Thus the Poisson's ratios ν_{13}^c and ν_{23}^c of a PE crystal unit became 0.029−0.038 and 0.090−0.096, respectively, by assuming the crystal lattice modulus along the chain axis to be 225 GPa.[3]

The Poisson's ratios ν_{13}^c and ν_{23}^c of a PE crystal unit were estimated by Miyasaka et al. for test specimens which were drawn up to 10 times and heat-treated at different temperatures.[9] These values became smaller with increasing heat-treated temperature indicating the increase in crystallinity and crystal size of the test specimens. The values of ν_{13}^c and those of ν_{23}^c are 1.6−3.4 and 2.4−3.8, respectively. It is evident that the value of Poisson's ratio must be lower than 0.5 for isotropic materials, while the values beyond 0.5 are generally acceptable for anisotropic system but the values reported by Miyasaka et al. seem to be too large to justify. Their abnormal large values are probably thought to be due to the fact that their test films were out of framework of homogeneous stress hypothesis.

Figures 4 and 5 show the crystal strain−stress relationship measured for the [200] and [002] directions of PVA, respectively. The plots also show a linear relationship in the given stress range. The plots are shown as the three examples assuring the good linear relationship. As discussed before, the negative crystal strain in the [200] direction and that in the [002] direction by the applied stress along the chain axis were used to determine the values of S_{13}^c and S_{23}^c, respectively. The measurements of S_{13}^c and S_{23}^c for the PVA films were much more difficult than those for the PE films, because of smaller peak shift and lower diffraction intensity. To assure the reproducibility, measurements were carried out for more than 30 test specimens. The diffraction intensity plots against twice the Bragg angles, however, were scattered at around a peak top for most of the specimens. Even so, the measurable

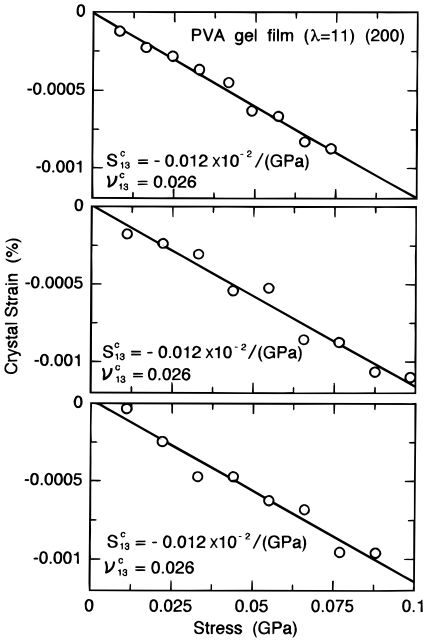

Figure 4. Crystal strain−stress relationship in the [200] direction for the PVA films, when the external stress is applied to the stretching direction.

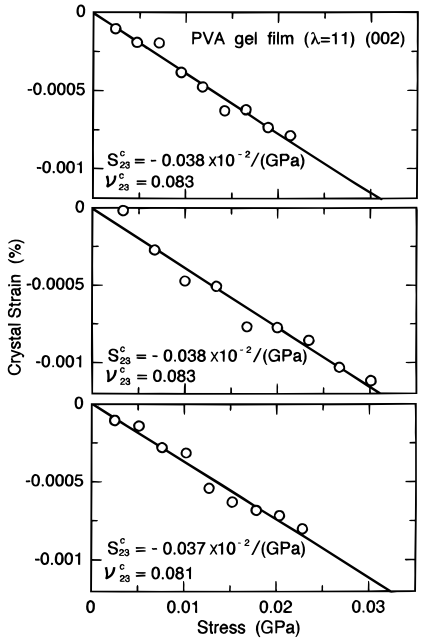

Figure 5. Crystal strain−stress relationship in the [002] direction for the PVA films, when the external stress is applied to the stretching direction.

Table 3. Reproducibility of S_{13}^c and S_{23}^c Obtained for the 7 PVA Test Specimens

S_{13}^c	$\times 10^{-2}$ GPa^{-1}	−0.010	−0.012	−0.014	
	frequency	1	5	1	
S_{23}^c	$\times 10^{-2}$ GPa^{-1}	−0.035	−0.037	−0.038	−0.041
	frequency	1	2	3	1

values for seven specimens took almost a constant value showing a good linear stress−strain relationship. Table 3 shows the reproducibility of the obtained values of S_{13}^c and S_{23}^c for the seven test specimens. The values of S_{13}^c and S_{23}^c were determined to be − 0.012 $\times 10^{-2}$ and (−0.037 to −0.038) $\times 10^{-2}$ GPa^{-1} respectively. The former and latter possibilities from Table 3 are about

70 and 85%, respectively. Using these values, the Poisson's ratios ν^c_{13} and ν^c_{23} of PVA crystals was calculated to be 0.026 and 0.081−0.083, respectively, by assuming the crystal lattice modulus in the chain direction to be 220 GPa.[8]

Let us compare the experimental values of S^c_{13} and S^c_{23} as measured by X-ray diffraction with corresponding theoretical values. For this purpose, we shall refer to theoretical values of S^{co}_{uv} calculated by Odajima et al.[24] and Tashiro et al.[25] at absolute temperature (−273 °C). Their theoretical values were reported as follows.

For PE by Odajima:[24]

$$S^{co}_{uv} = \begin{bmatrix} 21.4 & -2.76 & -0.150 & 0 & 0 & 0 \\ -2.76 & 12.0 & -0.246 & 0 & 0 & 0 \\ -0.150 & -0.246 & 0.396 & 0 & 0 & 0 \\ 0 & 0 & 0 & 3.53 & 0 & 0 \\ 0 & 0 & 0 & 0 & 128.2 & 0 \\ 0 & 0 & 0 & 0 & 0 & 48.5 \end{bmatrix} \times 10^{-2}\ \mathrm{GPa}^{-1}$$

For PE by Tashiro et al.:[25]

$$S^{co}_{uv} = \begin{bmatrix} 14.48 & -4.78 & -0.02 & 0 & 0 & 0 \\ -4.78 & 11.67 & -0.06 & 0 & 0 & 0 \\ -0.02 & -0.06 & 0.32 & 0 & 0 & 0 \\ 0 & 0 & 0 & 31.31 & 0 & 0 \\ 0 & 0 & 0 & 0 & 61.86 & 0 \\ 0 & 0 & 0 & 0 & 0 & 27.6 \end{bmatrix} \times 10^{-2}\ \mathrm{GPa}^{-1}$$

For PVA by Tashiro et al.:[25]

$$S^{co}_{uv} = \begin{bmatrix} 6.87 & -3.98 & -0.03 & 0 & 0 & -5.04 \\ -3.98 & 10.90 & -0.08 & 0 & 0 & 0.73 \\ -0.03 & -0.08 & 0.35 & 0 & 0 & 0.07 \\ 0 & 0 & 0 & 9.28 & -0.68 & 0 \\ 0 & 0 & 0 & 0 & 61.05 & 0 \\ -5.04 & 0.73 & 0.07 & 0 & 0 & 27.6 \end{bmatrix} \times 10^{-2}\ \mathrm{GPa}^{-1}$$

where S^{co}_{33} *denotes the crystal elastic compliance in the chain direction corresponding to the c axis for PE and the b axis for PVA, respectively.*

Here it should be noted that the absolute values of S^{co}_{13} and S^{co}_{23} calculated by using B matrix are higher than the experimental values measured at room temperature. For PE, the experimental values for S^c_{13} and S^c_{23} are fairly in good agreement with the theoretical values by Tashiro et al., rather than those by Odajima et al.[24] while the crystal lattice modulus ($1/S^{co}_{33}$) along the chain axis by Tashiro et al.[25] is beyond 300 GPa which is much higher than the experimental results (220−235 GPa)[1−3] measured by X-ray diffraction. The value, 253 GPa, calculated by Odajima et.[24] is fairly in good agreement with the experimental value. In the previous paper,[12] the numerical results for PE crystal lattice modulus were almost independent of the morphology for the PE dry gel films whose crystallinity is higher than 90%, and the second-order orientation factors are almost unity. For PVA crystals, the experimental values of S^c_{13} and S^c_{23} and their theoretical values by Tashiro et al.[25] are the same order and the experimental values of S^c_{33} by Matsuo et al.[8] are in good agreement with the theoretical one.[25] The big problem is the comparison between the results measured at room temperature and the theoretical ones at absolute temperature. Actually, experimental result of ($1/S^c_{33}$) at −160 °C lower than glass transition temperature reached 254 GPa[26] which is close to the values calculated by Odajima et al.[24] and Tashiro et al.[25] In accordance with drastic improvement of force field study, the theoretical values of elastic compliance S^{co}_{uv} of PE were obtained at room temperature. Lacks and Rutledge made the following estimation for the compliances at room temprature: $S^{co}_{13} = -0.087 \times 10^{-2}$, $S^{co}_{23} = -0.188 \times 10^{-2}$, $S^{co}_{33} = 0.35 \times 10^{-2}\ \mathrm{GPa}^{-1}$.[27] In this case, the chain modulus corresponds to 285 GPa. Recent molecular dynamics calculation by Zehnder resulted in the following compliance matrix of PE at 27 °C.[28]

$$S^{co}_{uv} = \begin{bmatrix} 28.1 & -16.1 & -0.036 & 0 & 0 & 0 \\ -17.2 & 25.8 & -0.41 & 0 & 0 & 0 \\ -0.088 & -0.36 & 0.462 & 0 & 0 & 0 \\ 0 & 0 & 0 & 47.4 & 0 & 0 \\ 0 & 0 & 0 & 0 & 59.9 & 0 \\ 0 & 0 & 0 & 0 & 0 & 43.1 \end{bmatrix} \times 10^{-2}\ \mathrm{GPa}^{-1}$$

where the chain modulus becomes 216 GPa. This value is almost equal to the experimental value measured by ultradrawn PE films.[3]

The experimental values of S^c_{13} and S^c_{23} for PE and PVA crystals were estimated using high drawn films assuming the stress homogeneous hypothesis. At present, the experiments for crystalline polymers except PE, PVA, and it-PP are very difficult because of poor drawability. Even so, measurements of Poisson's ratio for various crystalline polymers must be taken into consideration in further studies by using ultra-drawn films in order to study the intrinsic properties of the polymer crystal.

A question arises as to whether elastic compliances S^c_{13} and S^c_{23} as measured by X-ray diffraction are equal to their intrinsic (real) compliances S^{co}_{13} *and* S^{co}_{23}. The same question has also arisen for the Poisson ratios of a crystal unit. To derive the essential answer from the question, the compliances, S^c_{13} and S^c_{23}, and the Poisson ratios, ν^c_{13} and ν^c_{23}, must be analyzed in relation to morphology of the test specimens. Here, we shall refer to mathematical representation for estimating crystal lattice strains along and perpendicular to the chain axis as well as for estimating bulk strains along and perpendicular to external applied stress. The mathematical representation is discussed in terms of the geometrical arrangement as revealed by X-ray analysis.

Figure 6 shows a composite structural unit, in which oriented crystallites are surrounded by amorphous phases as a general case.[13,29−31] This model is employed as a tool to calculate the average elastic compliance in bulk and to formulate the stress−strain field in bulk. Assuming that the crystal unit is set in this field, the crystal strains can be represented as a function of composite mode and molecular orientation. Volume

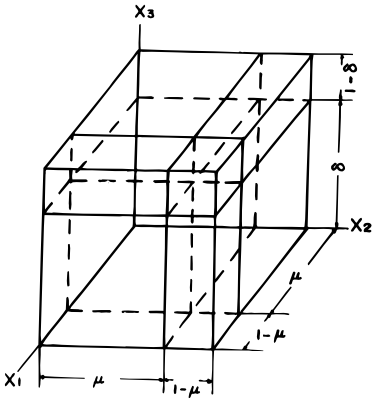

Figure 6. Composite structural unit of a semicrystalline polymer whose crystallites are surrounded by amorphous phase.

crystallinity X_c is represented by $\delta\mu^2$ by the use of the fraction lengths δ and μ in the directions of X_3 and X_2 (and X_1) axes. In this model system, amorphous layers are adjacent to the oriented crystalline layers with the interfaces perpendicular to the X_1, X_2, and X_3 axes. Strains of the two phases at the boundary are assumed to be identical. This model can be constructed by following three processes. First, an anisotropic amorphous layer lies adjacent to the crystallite with the interface perpendicular to the X_3 axes, and the resultant system is termed as phase I. Second, an anisotropic amorphous layer with fraction length $1 - \mu$ is attached to the structure of phase I in a plane normal to the X_1 direction to construct phase II. The final phase, III, can be constructed by adding an anisotropic amorphous layer with fraction length $1 - \mu$ to phase II. This procedure was represented elsewhere in detail.[13] It is well-known, of course, that at $\mu = 1$, this model corresponds to a series model, while at $\delta = 1$, it corresponds to a parallel model. In the following discussion, some final equations are described to shorten this paper. A complicated mathematical derivation was eliminated, since such treatment is similar to that of the crystal lattice modulus reported elsewhere.[8,12,13,29−31]

In accordance with the mathematical procedure of the generalized Hook's law, the bulk strain ϵ_{33} (σ, ΔT) can be represented as a function of external applied stress σ and temperature difference $\Delta T = T - T_0$ as follows:

$$\epsilon_{33}(\sigma,\Delta T) = \epsilon_{33}(\sigma) + \epsilon_{33}(\Delta T) \tag{3}$$

where T and T_0 are the measurable and reference temperatures. Namely, $\epsilon_{33}(\sigma,\Delta T)$ can be classified into two components: one is $\epsilon_{33}(\sigma)$ associated with the external applied stress, and the other, $\epsilon_{33}(\Delta T)$, is associated with the thermal expansion effect. That is

$$\epsilon_{33}(\sigma) = S^{B}_{33}\sigma_{33} = \frac{G}{C}\sigma_{33} \tag{4}$$

and

$$\epsilon_{33}(\Delta T) = \alpha^{B}_{33}\Delta T = \left(H - \frac{DG}{C}\right)\Delta T \tag{5}$$

where S^{B}_{33} is the bulk compliance in the stretching direction and α^{B}_{33} is the corresponding thermal expansion coefficient. The coefficients C, D, G, and H in eqs 4 and 5 are given by

$$C = \mu + \frac{(1-\mu)\left[\left(S^{II}_{13} + \frac{\mu S^{av}_{13}}{1-\mu}\right)S^{II}_{13} - \left(S^{II}_{11} + \frac{\mu S^{av}_{13}}{1-\mu}\right)S^{II}_{33}\right]}{\left(S^{II}_{13} + \frac{\mu S^{av}_{13}}{1-\mu}\right)S^{av}_{13} - \left(S^{II}_{11} + \frac{\mu S^{av}_{13}}{1-\mu}\right)S^{av}_{33}} \tag{6}$$

$$D = \frac{(1-\mu)\left[\left(S^{II}_{11} + \frac{\mu S^{av}_{11}}{1-\mu}\right)(\alpha^{av}_{33} - \alpha^{II}_{33}) - \left(S^{II}_{13} + \frac{\mu S^{av}_{13}}{1-\mu}\right)(\alpha^{av}_{11} - \alpha^{II}_{11})\right]}{\left(S^{II}_{13} + \frac{\mu S^{av}_{13}}{1-\mu}\right)S^{av}_{13} - \left(S^{II}_{11} + \frac{\mu S^{av}_{13}}{1-\mu}\right)S^{av}_{33}} \tag{7}$$

$$G = S^{II}_{33} + \frac{S^{II}_{13}(S^{II}_{13}\,S^{av}_{33} - S^{II}_{33}\,S^{av}_{13})}{\left(S^{II}_{13} + \frac{\mu}{1-\mu}S^{av}_{13}\right)S^{av}_{13} - \left(S^{II}_{11} + \frac{\mu}{1-\mu}S^{av}_{11}\right)S^{av}_{33}} \tag{8}$$

and

$$H = \frac{S^{II}_{13}\{S^{av}_{13}(\alpha^{av}_{33} - \alpha^{II}_{33}) - S^{av}_{33}(\alpha^{av}_{11} - \alpha^{II}_{11})\}}{\left(S^{II}_{13} + \frac{\mu}{1-\mu}S^{av}_{13}\right)S^{av}_{13} - \left(S^{II}_{11} + \frac{\mu}{1-\mu}S^{av}_{11}\right)S^{av}_{33}} \tag{9}$$

where S^{II}_{ij} and α^{II}_{ij} are elastic compliances and thermal expansion coefficients of phase II (see ref 13), respectively and S^{av}_{ij} are average elastic compliances of the amorphous phases. For example, S^{II}_{ij} can be represented by using intrinsic elastic compliances of the crystal and the amorphous phases, the fraction length (δ and μ) and the second and fourth order orientation factors of the crystal chain axes and the amorphous chain segments. All the detailed mathematical treatment were described elesewhere.[12,13,31]

The bulk strain $\epsilon_{11}(\sigma,\Delta T)$ in the X_1 direction can be represented as a function of σ and ΔT, when the external stress is applied in the X_3 direction. That is

$$\epsilon_{11}(\sigma,\Delta T) = \epsilon_{11}(\sigma) + \epsilon_{11}(\Delta T) \tag{10}$$

where

$$\epsilon_{11}(\sigma) = S^{B}_{13}\sigma_{33} = \frac{J}{\{\mu + (1-\mu)A\}C}\sigma_{33} \tag{11}$$

and

$$\epsilon_{11}(\Delta T) = \left[N - \frac{J}{\mu + (1-\mu)A}\left\{(1-\mu)B - \frac{D}{C}\right\}\right]\Delta T \tag{12}$$

Coefficients A, B, J, and N in eqs 11 and 12 are given

by

$$A = \frac{\left(S_{13}^{I} + \frac{\mu S_{13}^{av}}{1-\mu}\right)S_{13}^{I} - \left(S_{11}^{I} + \frac{\mu S_{11}^{av}}{1-\mu}\right)S_{33}^{I}}{\left(S_{13}^{I} + \frac{\mu S_{13}^{av}}{1-\mu}\right)S_{13}^{av} - \left(S_{11}^{I} + \frac{\mu S_{11}^{av}}{1-\mu}\right)S_{33}^{av}} \quad (13)$$

$$B = \frac{\left(S_{11}^{I} + \frac{\mu S_{11}^{av}}{1-\mu}\right)(\alpha_{33}^{av} - \alpha_{33}^{I}) - \left(S_{13}^{I} + \frac{\mu S_{13}^{av}}{1-\mu}\right)(\alpha_{11}^{av} - \alpha_{11}^{I})}{\left(S_{13}^{I} + \frac{\mu}{1-\mu}S_{13}^{av}\right)S_{13}^{av} - \left(S_{11}^{I} + \frac{\mu}{1-\mu}S_{11}^{av}\right)S_{33}^{av}} \quad (14)$$

$$J = \mu S_{13}^{I} + (1-\mu)S_{13}^{av}A + \frac{\mu(S_{12}^{I} - S_{12}^{av})(S_{13}^{I} S_{33}^{av} - S_{33}^{I} S_{13}^{av})}{\left(S_{13}^{I} + \frac{\mu}{1-\mu}S_{13}^{av}\right)S_{13}^{av} - \left(S_{11}^{I} + \frac{\mu}{1-\mu}S_{11}^{av}\right)S_{33}^{av}} \quad (15)$$

and

$$N = \mu\alpha_{11}^{I} + (1-\mu)\alpha_{11}^{av} + (1-\mu)S_{13}^{av} + (1-\mu)S_{13}^{av}B + \frac{\mu(S_{12}^{I} - S_{12}^{av})\{S_{13}^{av}(\alpha_{33}^{av} - \alpha_{33}^{I}) - S_{33}^{av}(\alpha_{11}^{av} - \alpha_{11}^{I})\}}{\left(S_{13}^{I} + \frac{\mu}{1-\mu}S_{13}^{av}\right)S_{13}^{av} - \left(S_{11}^{I} + \frac{\mu}{1-\mu}S_{11}^{av}\right)S_{33}^{av}} \quad (16)$$

where S_{ij}^{I} and α_{ij}^{I} are elastic compliances and thermal expansion coefficients of phase I, respectively. For example, S_{ij}^{I} can be represented by using intrinsic elastic compliances of the crystal phase and the second and fourth order orientation factors of crystallites. The detailed mathematical treatment was discussed elsewhere.[12,13,31]

The bulk strain $\epsilon_{22}(\sigma,\Delta T)$ in the X_2 direction can be also represented as a function of σ and ΔT, when external stress is applied in the X_3 direction. That is

$$\epsilon_{22}(\sigma,\Delta T) = \epsilon_{22}(\sigma) + \epsilon_{22}(\Delta T) \quad (17)$$

where

$$\epsilon_{22}(\sigma) = S_{23}^{B}\sigma_{33} = \left[S_{13}^{av} + \frac{\mu}{C}\{L(S_{12}^{II} - S_{12}^{av}) + (S_{23}^{II} - S_{13}^{av})\}\right]\sigma_{33} \quad (18)$$

and

$$\epsilon_{22}(\Delta T) = \left[\mu\alpha_{33}^{II} + (1-\mu)\alpha_{11}^{av} + \frac{\mu D}{C}S_{13}^{av} + \mu(S_{12}^{II} - S_{12}^{av})\left(M - \frac{DL}{C}\right) - \frac{\mu D}{C}S_{23}^{II}\right]\Delta T \quad (19)$$

The coefficients L and M in eqs 18 and 19 are given by

$$L = \frac{(S_{13}^{II} S_{33}^{av} - S_{33}^{II} S_{13}^{av})}{\left(S_{13}^{II} + \frac{\mu}{1-\mu}S_{13}^{av}\right)S_{13}^{av} - \left(S_{11}^{II} + \frac{\mu}{1-\mu}S_{11}^{av}\right)S_{33}^{av}} \quad (20)$$

and

$$M = \frac{S_{13}^{av}(\alpha_{33}^{av} - \alpha_{33}^{II}) - S_{33}^{av}(\alpha_{11}^{av} - \alpha_{11}^{II})}{\left(S_{13}^{II} + \frac{\mu}{1-\mu}S_{13}^{av}\right)S_{13}^{av} - \left(S_{11}^{II} + \frac{\mu}{1-\mu}S_{11}^{av}\right)S_{33}^{av}} \quad (21)$$

Here it should be noted that S_{13}^{B} must be equal to S_{23}^{B}, although eqs 11 and 18 are written with two different forms apparently. This can be demonstrated by replacing S_{ij}^{I} and S_{ij}^{II} with S_{ij}^{co} and S_{ij}^{ao}. These results are not shown in this paper, since they are much too complicated to write explicitly.

Poisson's ratio ν_{13}^{B} ($=\nu_{23}^{B}$) of the bulk specimens is given by

$$\nu_{13}^{B} = -\frac{S_{13}^{B}}{S_{33}^{B}} = \nu_{23}^{B} = -\frac{S_{23}^{B}}{S_{33}^{B}} \quad (22)$$

Now we shall discuss the crystal strain as detected by X-ray diffraction for the specimen where crystallites are surrounded by amorphous layers as shown in Figure 6. In this model system, it is evident that crystal strains are dependent upon the morphology of the composite system. Through a somewhat complicated mathematical treatment, the crystal strains, ϵ_{11}^{c}, ϵ_{22}^{c}, and ϵ_{33}^{c}, of the structural unit of crystalline phase in the three principal directions can be represented as a function of σ_{33} and ΔT as follows:

$$\epsilon_{11}^{c} = U_1\sigma_{33} + V_1\Delta T$$

$$\epsilon_{22}^{c} = U_2\sigma_{33} + V_1\Delta T \quad (23)$$

$$\epsilon_{33}^{c} = U_3\sigma_{33} + V_3\Delta T$$

Here the coefficients U_i ($i = 1-3$) and V_i ($i = 1-3$) are written in the Appendix. For PE crystals, the coefficients U_1, U_2, and U_3 correspond to elastic compliances along the *a*, *b*,and *c* axis as measured by X-ray diffraction technique, respectively, and the coefficients V_1, V_2, and V_3 denote corresponding thermal expansion coefficients. On the other hand, *for PVA with a monoclinic crystal unit, U_1, U_2, and U_3 correspond to elastic compliances along the a axis, the [002] direction, and the b axis (crystal chain axis), respectively, and the V_1, V_2, and V_3 are corresponding thermal expansion coefficients.* Measurable crystal strain and thermal expansion in the [200] direction may be given by using the formula of transformation of strain components:

$$\epsilon_{[200]}^{c} = \sin^2\Phi\epsilon_{22}^{c} + \cos^2\Phi\epsilon_{11}^{c} = (U_1\cos^2\Phi + U_2\sin^2\Phi)\sigma_{33} + (V_1\cos^2\Phi + V_2\sin^2\Phi)\Delta T = S_{[200]}^{c}\sigma_{33} + \alpha_{[200]}^{c}\Delta T \quad (24)$$

Here Φ specifies the azimuthal angle between the [200] direction and the *a* axis. The coefficients $S_{[200]}^{c}$ and $\alpha_{[200]}^{c}$ correspond to the elastic compliance and thermal expansion coefficient in the [200] direction as measured by X-ray diffraction, respectively.

Using eq 23, the Poisson ratios ν_{13}^{c} and ν_{23}^{c} may be given by

$$\nu_{13}^{c} = -\frac{U_1}{U_3} \tag{25}$$

and

$$\nu_{23}^{c} = -\frac{U_2}{U_3} \tag{26}$$

To compare the calculated result with the experimental one, the Poisson ratio ν_{13}^{c} of PVA crystals is obliged to replace U_1 in eq 25 by the measurable elastic compliance $S_{[200]}^{c}$ in the [200] direction as follows:

$$\nu_{13}^{c} = -\frac{S_{[200]}^{c}}{U_3} \tag{27}$$

The above approximation is no problem, since the angle β (91.7°) within the crystal unit is close to 90°. Through eqs 3−27, the crystal Poisson ratios, ν_{13}^{c} and ν_{23}^{c}, as measured by X-ray diffraction are different from their intrinsic crystal Poisson ratios, ν_{13}^{co} and ν_{23}^{co}. To check the difference between measurable and intrinsic values, the values of intrinsic crystal elastic compliances S_{ij}^{co} are indispensable to calculate the bulk Poisson ratio ν_{13}^{B} (= ν_{23}^{B}) and the crystal Poisson ratios, ν_{13}^{c} and ν_{23}^{c} as measured by X-ray diffraction. At present, we adopted the values of S_{ij}^{co} for PE by Odajima et al.[24] and for PVA by Tashiro et al.[25] as the intrinsic (real) values in order to pursue numerical calculations.

The elastic compliances S_{ij}^{ao} of amorphous phase needed in the calculation are not precisely known. Following our crude approximation described elsewhere,[12,29−31] we estimated the elastic compliances S_{11}^{ao} and S_{22}^{ao} by double differentiation of Lennard−Jones potential energy functions, while the compliance S_{33}^{ao} was estimated by assuming that the modulus along the chain axis is proportional to the number of molecular chains in the unit area perpendicular to the chain axis.[8,12,31] Thus, we have

$$S_{11}^{ao} = S_{22}^{ao} = \left(\frac{\rho_c}{\rho_a}\right)^4 S_{11}^{c^t} \tag{28}$$

$$S_{33}^{ao} = \left(\frac{\rho_c}{\rho_a}\right) S_{33}^{c^t}$$

where the compliance $S_{11}^{c^t}$ and $S_{33}^{c^t}$ are given by[12]

$$S_{11}^{c^t} = \frac{1}{8}(3S_{11}^{co} + 3S_{22}^{co} + 2S_{12}^{co} + S_{66}^{co}) \tag{29}$$

$$S_{33}^{c^t} = S_{33}^{co}$$

Since the amorphous chain segment is uniaxially symmetric around the chain axis, the other compliances

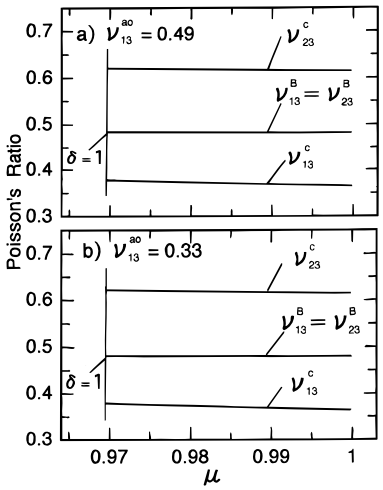

Figure 7. μ dependence of the crystal Poisson ratios, ν_{13}^{c} and ν_{23}^{c}, of PE and the μ dependence of the bulk Poisson ratio, ν_{13}^{B} (=ν_{23}^{B}), obtained for the perfect oriented system: (a) the curves calculated at $\nu_{13}^{ao} = 0.49$; (b) the curves calculated at $\nu_{13}^{ao} = 033$

can be estimated as[8,12,29]

$$S_{44}^{ao} = S_{55}^{ao}$$

$$S_{12}^{ao} = -\nu_{13}^{ao} S_{11}^{ao}$$

$$S_{23}^{ao} = S_{13}^{ao} = -\nu_{13}^{ao} S_{33}^{ao}$$

$$2S_{11}^{ao} = (2S_{13}^{ao} + S_{55}^{ao})\Omega$$

$$2S_{11}^{ao} = 2S_{12}^{ao} + S_{66}^{ao}$$

where Ω is set to be unity.[8,12] ν_{13}^{ao} (= ν_{23}^{ao}) is an unknown parameter and is set to be 0.49 or 0.33. The former or latter value of ν_{13}^{ao} (= ν_{23}^{ao}) is selected in the case where the mechanical property of the amorphous phase is similar to an ideal rubber elasticity or glassy state, respectively. Accordingly, the numerical calculation was done to check the morphology dependence on the values of ν_{13}^{c} and ν_{23}^{c} as estimated by X-ray diffraction in comparison with ν_{13}^{co} (= S_{13}^{co}/S_{33}^{co}) and ν_{23}^{co} (= S_{23}^{co}/S_{33}^{co}) estimated by Odajima et al. for PE[24] and Tashiro et al. for PVA.[25] Of course, this check is very important to obtain the information with regard to the validity of the experimental results shown in Figures 2−5. Here it should be noted that, in the present model system, the second- and fourth-order orientation factors and crystallinity were estimated experimentally, and consequently the composite structural unit of the crystal and amorphous phases must be taken into consideration as an unknown parameter. Accordingly, following analysis was done in this viewpoint.

Figure 7 shows the μ dependence of the crystal Poisson ratios ν_{13}^{c} and ν_{23}^{c} of PE as measured by X-ray diffraction and μ dependence of the Poisson ratio ν_{13}^{B} (= ν_{23}^{B}) in bulk, where columns a and b correspond to the results calculated at $\nu_{13}^{ao} = 0.49$ and 0.33, respectively. To check the outline of the μ dependence, calculations were carried out for the simple system where the orientation factors of the *c* axis and amorphous chain segments are unity denoting the perfect orientation with respect to the stretching direction. Crystallinity was set

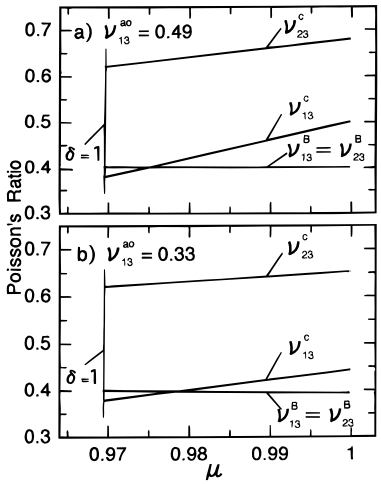

Figure 8. μ dependence of the crystal Poisson ratios, ν_{13}^{c} and ν_{23}^{c}, of PE and μ dependence of the bulk Poisson ratio, ν_{13}^{B} ($=\nu_{23}^{B}$), obtained for the experimental data listed in Table 1: (a) the curves calculated at $\nu_{13}^{ao} = 0.49$; (b) the curves calculated at $\nu_{13}^{ao} = 0.33$.

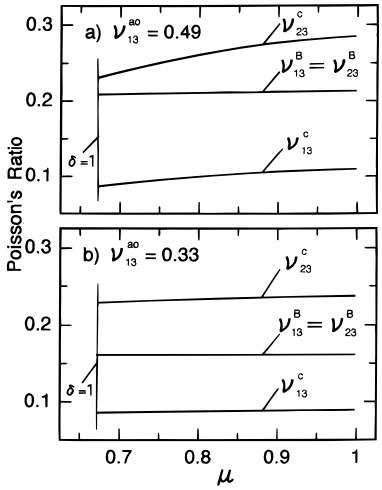

Figure 9. μ dependence of the crystal Poisson ratios, ν_{13}^{c} and ν_{23}^{c}, of PVA and μ dependence of the bulk Poisson ratio, ν_{13}^{B} ($=\nu_{23}^{B}$), obtained for the perfect oriented system: (a) the curves calculated at $\nu_{13}^{ao} = 0.49$; (b) the curves calculated at $\nu_{13}^{ao} = 0.33$.

to be 94% (see Table 1). The crystal and bulk Poisson ratios are almost independent of μ associated with the composite of the crystal and amorphous phases shown in Figure 6. At $\nu_{13}^{ao} = 0.49$, the values of ν_{13}^{c} and ν_{23}^{c} are 0.365−0.379 and 0.615−0.621, respectively, while at $\nu_{13}^{ao} = 0.33$, they are 0.364−0.379 and 0.613−0.621, respectively. This means that the ν_{13}^{ao} effect on ν_{13}^{c} and ν_{23}^{c} can be negligibly small because of the high crystallinity (93−95%) of the test PE films. Anyway, the above values of ν_{13}^{c} and ν_{23}^{c} are almost equal to the intrinsic values, 0.379 (ν_{13}^{co}) and 0.621 (ν_{23}^{co}), respectively, calculated by Odajima et al.[24] This result predicts that crystal Poisson's ratios as estimated by X-ray diffraction are almost equal to the corresponding intrinsic values, when crystal and amorphous chains are oriented perfectly with respect to the stretching direction and the measurable values become perfectly equal to the intrinsic values at $\mu = 0.9695$ ($\delta = 1$) denoting the parallel model in Figure 6.

Parts a and b of Figure 8 show the μ dependence of ν_{13}^{c} and ν_{23}^{c} and ν_{13}^{B} ($= \nu_{23}^{B}$) at $\nu_{13}^{ao} = 0.49$ and 0.33, respectively, for the test PE specimens. In addition to the crystallinity (94%), the second order orientation factors, F_{200}^{c} of the c-axis and F_{200}^{am} of the amorphous chain segments were set to be 0.925 and 0.856, respectively, from the experimental values listed in Table 1. As discussed in the Experimental Section, the fourth-order orientation factors of the *c* axis was calculated by using the orientation distribution functions of the *c* axis, while that of the amorphous chain segments was calculated by using an inversely superposed Gaussian type function with the parameter which gives the best value of F_{200}^{am}.[8,31] In comparison with Figure 7, it is evident that the μ dependence of ν_{13}^{c} and ν_{23}^{c} becomes significant with increasing orientational fluctuation of the *c* axis and that of amorphous chain segments. Namely, at $\nu_{13}^{ao} = 0.49$, ν_{13}^{c} and ν_{23}^{c} 0.379−0.501 and 0.621−0.681, respectively, while at $\nu_{13}^{ao} = 0.33$, they are 0.379−0.444 and 0.621−0.653, respectively. At $\mu = 0.9695$ ($\delta = 1$) denoting a parallel model in Figure 6, ν_{13}^{c} and ν_{23}^{c} as measured by X-ray diffraction are 0.379 and 0.621, respectively. Namely, they are equal to ν_{13}^{co} and ν_{23}^{co}, respectively. This tendency is quite different from the μ dependence of the crystal lattice modulus along the crystal chain axis. According to the previous paper,[8,12,31] the measurable crystal lattice modulus is almost equal to the corresponding intrinsic crystal lattice modulus at $\mu = 1$ denoting a series model in Figure 6. Figures 7 and 8 indicate that Poisson's ratio ν_{13}^{B} ($= \nu_{23}^{B}$) are almost independent of μ but the values become higher with increasing orientational degree of crystallites.

Figure 9 shows the μ dependence of ν_{13}^{c} and ν_{23}^{c} of PVA crystals as measured by X-ray diffraction and the μ dependence of ν_{13}^{B} ($=\nu_{23}^{B}$) of the bulk in the perfect oriented system, in which columns a and b correspond to the curves calculated at $\nu_{13}^{ao} = 0.49$ and 0.33, respectively. In this system, crystallinity was set to be 55% (see Table 1) and the μ dependence can be discussed only in relation to the composite mode. At $\nu_{13}^{ao} = 0.49$, ν_{13}^{c} and ν_{23}^{c} cause significant effect on μ and they increase with increasing μ. However, the μ dependence at $\nu_{13}^{ao} = 0.33$ is less effective than that at $\nu_{13}^{ao} = 0.49$. ν_{13}^{B} ($= \nu_{23}^{B}$) is almost independent of μ. At $\mu = 0.6708$ ($\delta = 1$) denoting the parallel model in Figure 6, the values of ν_{13}^{c} and ν_{23}^{c} are equal to those of ν_{13}^{co} and ν_{23}^{co}, respectively. Comparing the results in Figure 9 with those in Figure 7, the μ dependence of ν_{23}^{B} and ν_{23}^{c} appears even in the perfectly oriented system. This is obviously due to the lower crystallinity (52−58%) of the PVA test specimens in comparison with the PE specimens (93−95%). Incidentally, the μ dependence of ν_{13}^{B} ($= \nu_{23}^{B}$) is less sensitive in comparison with that of ν_{13}^{c} and ν_{23}^{c}.

Figure 10 shows the μ dependence of ν_{13}^{c}, ν_{23}^{c}, and ν_{13}^{B} ($= \nu_{23}^{B}$). In this calculation, the second-order orientation factors of the c axis and amorphous chain segments were selected to be 0.925 and 0.856, respectively, and the crystallinity was set to be 55% from the experimental results in Table 1. The fourth-order orientation factors of the *b* axis (crystal chain axis) were obtained by the same treatments as those for PE. It is seen that ν_{13}^{c} is almost constant against μ. In contrast, ν_{23}^{c} and ν_{13}^{B} ($= \nu_{23}^{B}$) calculated at $\nu_{13}^{ao} = 0.49$ slightly increase with

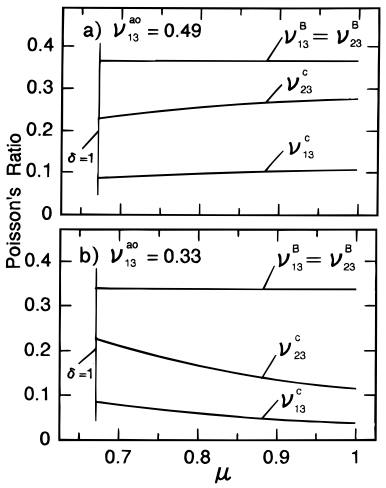

Figure 10. μ dependence of the crystal Poisson ratios, ν_{13}^{c} and ν_{23}^{c}, of PVA and μ dependence of the bulk Poisson ratio, ν_{13}^{B} (=ν_{23}^{B}), obtained for the experimental data listed in Table 1: (a) the curves calculated at $\nu_{13}^{ao} = 0.49$; (b) the curves calculated at $\nu_{13}^{ao} = 0.33$.

increasing μ, while they decrease at $\nu_{13}^{ao} = 0.33$. Incidentally, ν_{13}^{c} and ν_{23}^{c} are equal to ν_{13}^{co} and ν_{23}^{co}, respectively, at $\mu = 0.6708$ ($\delta = 1$) denoting a parallel model.

Through a series of the numerical calculations in Figures 7−10, it turns out that the crystal Poisson ratios, ν_{13}^{c} and ν_{23}^{c}, as estimated by X-ray diffraction, are almost equal to the intrinsic (real) Poisson ratio, when the composite of the crystalline and amorphous phases within a bulk specimen can be represented as a parallel model. In contrast, the values of ν_{13}^{c} and ν_{23}^{c} slightly deviate from the intrinsic values, when the morphology of a test specimen can be represented as a series model. This tendency is quite different from the results obtained for the crystal lattice modulus as measured by X-ray diffraction.[8,12] This is due to the fact that the crystal strain in the transverse direction can be detected as the intrinsic (real) crystal strain by X-ray diffraction, when the composite of the crystal and amorphous phases is represented as a parallel model with respect to the stretching direction. That is, in the transverse direction, the crystal strain is independent of the amorphous strain, since a parallel model with respect to the stretching direction correspond to a series model with respect to the transverse direction. Certainly, the composite modes of the PE and PVA films used as test specimens are similar to a series model as discussed in the previous paper.[3,8,12,31] Nevertheless, we must emphasize that X-ray diffraction plays an important role to measure the elastic compliance and Poisson's ratios of PE and PVA crystals. This is because the numerical results in Figures 7−10 showed very small μ dependence of the crystal Poisson ratios assuring the validity of the measurable values, even if the morphology of the test specimens used in this experiment is represented as a series model with respect to the stretching direction. This means that the validity increases as crystallinity and molecular orientational degree of test specimens increase. Incidentally, as shown in Figures 7−10, the Poisson ratio in bulk is independent of the composite mode shown in Figure 6, but the value depends on the orientational degree of crystallites and amorphous chain segments.

IV. Conclusion

From the above consideration, two main conclusions can be drawn.

First, elastic compliances S_{13}^{c} and S_{23}^{c} of PE and PVA were measured by X-ray diffraction. Drawn PE films with $\lambda = 60$ and PVA films with $\lambda = 11$ were used as test specimens. The values of S_{13}^{c} and S_{23}^{c} for PE crystals were (−0.013 to −0.017) × 10^{-2} and (−0.040 to −0.043) × 10^{-2} GPa^{-1}, respectively, while those of S_{13}^{c} and S_{23}^{c} for PVA crystals are −0.012 × 10^{-2} and (−0.037 to −0.038) × 10^{-2} GPa^{-1}, respectively. The absolute value of S_{13}^{c} for PVA crystals was the lowest. The corresponding Poisson ratios, ν_{13}^{c} and ν_{23}^{c}, of PE crystals were 0.029−0.038 and 0.090−0.096, respectively, while the corresponding Poisson ratios, ν_{13}^{c} and ν_{23}^{c}, of PVA crystals are 0.026 and 0.081−0.083.

Secondly, one of approaches was proposed for estimating the crystal Poisson ratios of semicrystalline polymers as a function of crystallinity, chain orientation and composite mode of crystal and amorphous phases. Mathematical description indicated that the Poisson ratios as measured by X-ray diffraction are different from their intrinsic crystal Poisson ratios. Even so, the numerical values were almost same, when the composite of the crystal and amorphous phases was represented as a parallel model. In contrast, the measurable values slightly deviate from the intrinsic ones in a series model.

Appendix

The coefficients U_i ($i = 1-3$) and V_i ($i = 1-3$) in eq 23 may be given by

$$U_1 = \frac{(-\mathrm{FA1} + S_{13}^{co})}{C[\mu + (1-\mu)A]} \tag{A-1}$$

$$U_2 = \frac{(-\mathrm{FB1} + S_{23}^{co})}{C[\mu + (1-\mu)A]} \tag{A-2}$$

$$U_3 = \frac{(-\mathrm{FC1} + S_{33}^{co})}{C[\mu + (1-\mu)A]} \tag{A-3}$$

$$V_1 = -\frac{(-\mathrm{FA1} + S_{13}^{co})[BC(1-\mu) + D]}{C[\mu + (1-\mu)A]} - \mathrm{FA2} + \alpha_{11}^{co} \tag{A-4}$$

$$V_2 = -\frac{(-\mathrm{FB1} + S_{23}^{co})[BC(1-\mu) + D]}{C[\mu + (1-\mu)A]} - \mathrm{FB2} + \alpha_{22}^{co} \tag{A-5}$$

$$V_3 = -\frac{(-\mathrm{FC1} + S_{33}^{co})[BC(1-\mu) + D]}{C[\mu + (1-\mu)A]} - \mathrm{FC2} + \alpha_{33}^{co} \tag{A-6}$$

where the coefficients FA1, FA2, FB1, FB2, FC1, and

FC2 in eqs A-1−A-6 are given by

$$\mathrm{FA1} = \frac{(S_{13}^{cv} - S_{13}^{av})(S_{11}^{co} + S_{12}^{co})}{S_{11}^{cv} + S_{12}^{cv} + \frac{\delta}{1-\delta}(S_{11}^{av} + S_{12}^{av})} \quad \text{(A-7)}$$

$$\mathrm{FA2} = \frac{(\alpha_{11}^{cv} - \alpha_{11}^{av})(S_{11}^{co} + S_{12}^{co})}{S_{11}^{cv} + S_{12}^{cv} + \frac{\delta}{1-\delta}(S_{11}^{av} + S_{12}^{av})} \quad \text{(A-8)}$$

$$\mathrm{FB1} = \frac{(S_{13}^{cv} - S_{13}^{av})(S_{12}^{co} + S_{22}^{co})}{S_{11}^{cv} + S_{12}^{cv} + \frac{\delta}{1-\delta}(S_{11}^{av} + S_{12}^{av})} \quad \text{(A-9)}$$

$$\mathrm{FB2} = \frac{(\alpha_{11}^{cv} - \alpha_{11}^{av})(S_{12}^{co} + S_{22}^{co})}{S_{11}^{cv} + S_{12}^{cv} + \frac{\delta}{1-\delta}(S_{11}^{av} + S_{12}^{av})} \quad \text{(A-10)}$$

$$\mathrm{FC1} = \frac{(S_{13}^{cv} - S_{13}^{av})(S_{13}^{co} + S_{23}^{co})}{S_{11}^{cv} + S_{12}^{cv} + \frac{\delta}{1-\delta}(S_{11}^{av} + S_{12}^{av})} \quad \text{(A-11)}$$

$$\mathrm{FC2} = \frac{(\alpha_{11}^{cv} - \alpha_{11}^{av})(S_{13}^{co} + S_{23}^{co})}{S_{11}^{cv} + S_{12}^{cv} + \frac{\delta}{1-\delta}(S_{11}^{av} + S_{12}^{av})} \quad \text{(A-12)}$$

References and Notes

(1) Sakurada, I.; Nukushina, Y.; Ito, T. *J. Polym. Sci.* **1962**, *57*, 651.
(2) Sakurada, I.; Ito, T.; Nakamae, K. *J. Polym. Sci. Part C* **1966**, *15*, 75.
(3) Matsuo, M.; Sawatari, C. *Macromolecules* **1986**, *19*, 2036.
(4) Matsuo, M.; Sawatari, C. *Macromolecules* **1988**, *21*, 1658.
(5) Strobl, G. R.; Eckel, R. *J. Polym. Sci., Polym. Phys. Part C* **1976**, *14*, 913.
(6) Holliday, L.; White, J. W.; *Pure Appl. Chem.* **1971**, *26*, 545.
(7) Sawatari, C.; Matsuo, M. *Macromolecules* **1986**, *19*, 2653.
(8) Matsuo, M.; Harashina, Y.; Ogita, T. *Polym. J.* **1993**, *25*, 319.
(9) Miyasaka, K.; Makishima, K. *Kobunshi Ronbunshu* **1966**, *23*, 785.
(10) Nakamae, K.; Nishino, T.; Airu, X. *Polymer* **1992**, *33*, 4898.
(11) Tashiro, K.; Nishimura, T.; Kobayashi, M. *Macromolecules* **1996**, *29*, 8188.
(12) Sawatari, C.; Matsuo, M. *Macromolecules* **1986**, *19*, 2726.
(13) Matsuo, M. *Macromolecules* **1990**, *23*, 3261.
(14) Lee, Y.-L.; Bretzlaff, R.S.; Wool R.P. *Macromolecules* **1983**, *16*, 5964.
(15) Wool, R. P.; Bretzlaff, R. S.; Li, B. Y.; Wang, C. H.; Boyd, R. H. *J. Polym. Sci., Part B, Polym. Phys.* **1986**, *24*, 1039.
(16) Smith, P.; Lemstra, P. J. *J. Mater. Sci.* **1980**, *15*, 505.
(17) Smith, P.; Lemstra, P. J. Pipjers, J. P. L.; Kiel, A. M. *Colloid Polym. Sci.* **1981**, *258*, 1070.
(18) Stein, R. S.; Norris, F. H. *J. Polym. Sci.* **1956**, *21*, 381.
(19) Kang, S. J.; Matsuo, M. *Polymer J.* **1989**, *21*, 49.
(20) Cha, W. I.; Hyon, S. H.; Ikada, Y. *J. Polym. Sci., Part B: Polym. Phys.* **1994**, *32*, 297.
(21) Sawatari, C.; Yamamoto, Y.; Yanagida, N.; Matsuo, M. *Polymer* **1993**, *43*, 956.
(22) Ogita, T.; Sakabe, T.; Tyamada, T.; Sano, H.; Noguchi, H.; Xu, C. Y.; Matsuo, M. *Colloid Polym. Sci.* **1996**, *274*, 928.
(23) Keller, A. *Growth and Perfection of Crystals*; Turnbell, D., Ed.; John Wiley & Sons, New York 1958.
(24) Odajima, A.; Maeda, T. *J. Polym. Sci. Part C* **1966**, *15*, 55.
(25) Tashiro, K.; Kobayashi, M.; Tadokoro, H. *Macromolecules* **1978**, *11*, 914.
(26) Nishino, T.; Ohbubo, H.; Nakamae, K. *J. Macromol. Sci., Phys.* **1992**, *B31*, 191.
(27) Lacks, D. J.; Rutledge, G. C. *J. Phys. Chem.* **1994**, *98*, 1222.
(28) Zehnder, M. Atomic Simulation of the Elasticity of Polymers. PhD. Thesis ETH-Zurich, 1997.
(29) Hibi, S.; Maeda, M.; Makino, S.; Nomura, S.; Kawai, H. *Sen-i-Gakkaishi* **1973**, *29*, 79.
(30) Maeda, M.; Hibi, S.; Itoh, F.; Nomura, S.; Kawaguchi, T.; Kawai, H. *J Polym. Sci., Part A-2.* **1970**, 8, 1303.
(31) Matsuo, M.; Satoh, R.; Shimizu, Y. *Colloid Polym. Sci.* **1993**, *271*, 11.

MA980214P